

Systemic administration of mesenchymal stem cells loaded with a novel oncolytic adenovirus carrying a bispecific T cell engager against hepatocellular carcinoma

Xiangfei Yuan^{a†}, Yang Lu^{b†}, Yuanyuan Yang^{c†}, Wencong Tian^d, Dongmei Fan^b, Ruoqi Liu^b, Xiaomin Lei^b, Yafei Xia^e, Lei Yang^a, Shu Yan^e, and Dongsheng Xiong^b

^aTianjin Key Laboratory of Acute Abdomen Disease Associated Organ Injury and ITCWM Repair, Tianjin Medical University Nankai Hospital, Tianjin, China; ^bState Key Laboratory of Experimental Hematology, National Clinical Research Center for Blood Diseases, Haihe Laboratory of Cell Ecosystem, Institute of Hematology & Blood Diseases Hospital, Chinese Academy of Medical Sciences & Peking Union Medical College, Tianjin, China; ^cDepartment of Pharmacy, Tianjin Medical University General Hospital, Tianjin, China; ^dDepartment of General Surgery, Tianjin Union Medical Center, Tianjin, China; ^eDepartment of Pharmacy, Integrated Chinese and Western Medicine Hospital, Tianjin University, Tianjin, China

ABSTRACT

We previously established a hepatocellular carcinoma (HCC) targeting system of conditionally replicative adenovirus (CRAd) delivered by human umbilical cord-derived mesenchymal stem cells (HUMSCs). However, this system needed to be developed further to enhance the antitumor effect and overcome the limitations caused by the alpha-fetoprotein (AFP) heterogeneity of HCC. In this study, a bispecific T cell engager (BiTE) targeting programmed death ligand 1 controlled by the human telomerase reverse transcriptase promoter was armed on the CRAd of the old system. It was demonstrated on orthotopic transplantation model mice that the new system had a better anti-tumor effect with no more damage to extrahepatic organs and less liver injury, and the infiltration and activation of T cells were significantly enhanced in the tumor tissues of the model mice treated with the new system. Importantly, we confirmed that the new system eliminated the AFP-negative cells on AFP heterogeneous tumor models efficiently. Conclusion: Compared with the old system, the new system provided a more effective and safer strategy against HCC.

ARTICLE HISTORY

Received 8 November 2022
Revised 25 May 2023
Accepted 25 May 2023

KEYWORDS

AFP; BiTE; Crad; HCC; hepatic differentiation; HUMSC; PBMC; PD-L1; tumor heterogeneity





Background

Hepatocellular carcinoma (HCC) is a leading cause of cancer-related death in many parts of the world¹. The 5-year survival rate of patients with HCC is low due to the high rate of recurrence and metastasis of HCC and resistance to antitumor drugs². Recently, many novel strategies have emerged to develop the treatment of HCC^{3–5}. In our previous studies, an HCC-targeting system of conditionally replicative adenovirus (CRAd) delivered by human umbilical cord – derived mesenchymal stem cells (HUMSCs) was established, which depended on the homing and hepatic differentiation of HUMSCs at tumor sites and the specific transcriptional activity of the alpha-fetoprotein (AFP) promoter in differentiated HUMSCs and hepatoma cells⁶. However, we thought that the anti-tumor effect of this system should be strengthened. Additionally, AFP heterogeneity in hepatoma tissues was a challenge to the clinical application of this targeting system because the CRAd selectively cleared the AFP-positive tumor cells but not the negative ones. Therefore,


the targeting system needed to be developed by arming it with an additional antitumor element.

In recent years, the oncolytic adenovirus armed with a bispecific T cell engager (BiTE) has been investigated for treating many solid tumors^{7–9}. BiTE is a chimeric protein composed of two single-chain variable fragments (scFvs) connected with a flexible peptide linker, one specific for tumor-associated antigen and the other for CD3¹⁰. Oncolytic virotherapy can evoke antitumor immune responses and increase the intratumoral infiltration of T lymphocytes^{11–13}. When BiTE is armed, the intratumoral T cells can be activated and can selectively eliminate tumor cells. Consequently, these properties of oncolytic adenovirus and BiTE are ideal for combinatorial approaches.

We used αCD3HAC, a BiTE specific for programmed death ligand 1 (PD-L1) and CD3, for treating triple-negative breast cancer (TNBC) by blocking PD-L1 and activating T cells¹⁴. Similar to TNBC, HCC was characterized by high expression of PD-L1^{15,16} so that a cistron constructed by human telomerase reverse transcriptase

CONTACT Xiangfei Yuan  yuanxiangfei100@163.com  Tianjin Key Laboratory of Acute Abdomen Disease Associated Organ Injury and ITCWM Repair, Tianjin Medical University Nankai Hospital, No. 6, Changjiang Road, Tianjin 300100, China; Shu Yan  13389989966@163.com  Department of Pharmacy, Integrated Chinese and Western Medicine Hospital, Tianjin University, No. 6, Changjiang Road, Tianjin 300100, China; Dongsheng Xiong  dsxiong@ihcams.ac.cn  State Key Laboratory of Experimental Hematology, National Clinical Research Center for Blood Diseases, Haihe Laboratory of Cell Ecosystem, Institute of Hematology & Blood Diseases Hospital, Chinese Academy of Medical Sciences & Peking Union Medical College, 288 Nanjing Road, Tianjin 300020, China

[†]Xiangfei Yuan, Yang Lu and Yuanyuan Yang shared co-first authorship.

 Supplemental data for this article can be accessed online at <https://doi.org/10.1080/2162402X.2023.2219544>

© 2023 The Author(s). Published with license by Taylor & Francis Group, LLC.

This is an Open Access article distributed under the terms of the Creative Commons Attribution-NonCommercial License (<http://creativecommons.org/licenses/by-nc/4.0/>), which permits unrestricted non-commercial use, distribution, and reproduction in any medium, provided the original work is properly cited. The terms on which this article has been published allow the posting of the Accepted Manuscript in a repository by the author(s) or with their consent.

(hTERT) promoter and α CD3HAC coding sequence was loaded on the CRAd to improve the old targeting system. In this study, the new system was investigated in terms of exerting a synergistic antitumor effect and overcoming AFP heterogeneity.

Materials and methods

Cell lines and cell culture

Human hepatoma cell lines (HepG2 and SMMC-7721), embryonic renal cell line 293 A, and human embryonic kidney cell-derived 293T cell line (Institute of Hematology and Blood Diseases Hospital Chinese Academy of Medical Sciences and Peking Union Medical College, PUMC, Tianjin, China), were maintained in DMEM (#1791922, Gibco, USA) supplemented with 10% FBS (#10099-141, Gibco, USA). Human T cell leukemia cell-line Jurkat (Institute of Hematology and Blood Diseases Hospital Chinese Academy of Medical Sciences and Peking Union Medical College) was maintained in RPMI 1640 (#1721503, Gibco, USA) plus 10% FBS.

Preparation of adenoviruses

The construction of adenoviruses was based on the AdEasy adenoviral vector system (#240009, Stratagene, USA) and is shown in Figure 1a. The plasmid pAdTrack and pAdE1A were established previously⁶. The tandem sequences of hTERT promoter and α CD3HAC were inserted into pAdTrack and pAdE1A, respectively, at the sites of *KpnI* and *BglIII*. Later, all the four shuttle vectors (pAdTrack, pAdE1A, pAd α CD3HAC, and pAdE1A- α CD3HAC) were packaged using the methods described previously⁶. The titers were determined using a 50% tissue culture infectious dose (TCID50).

Isolation, culture and hepatic differentiation of HUMSCs

HUMSCs were isolated from the gelatinous Wharton's jelly within the human umbilical cord. The methods of isolation, culture and hepatic differentiation were described previously^{6,14,17}.

Luciferase assay for AFP and hTERT promoters in vitro

The pGL3-AFP promoter and pGL3-hTERT promoter were constructed previously. The transcriptional activities in HepG2 and

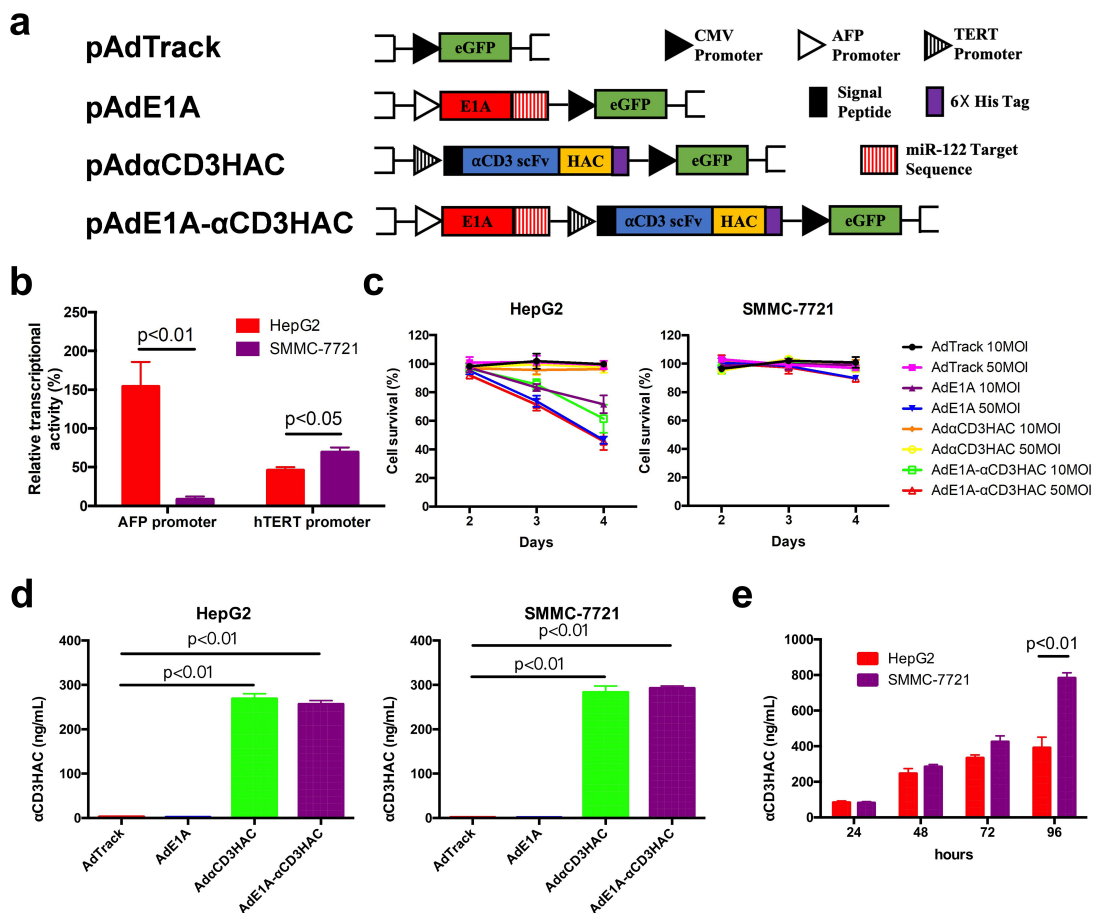


Figure 1. Identification of the novel CRAd armed with α CD3HAC. (a) Schematic representations of the novel CRAd (AdE1A- α CD3HAC) and its control adenoviruses. (b) Transcriptional activities of the AFP promoter and the hTERT promoter in HepG2 and SMMC-7721 cell lines, respectively, detected by the dual-luciferase reporter system. (c) Viabilities of HepG2 and SMMC-7721 cells after infection with different adenoviruses at 10 or 50 MOI measured using CCK-8 assays. (d) Concentrations of α CD3HAC in the culture supernatants of HepG2 and SMMC-7721 cells infected with different adenoviruses at 50 MOI for 48 h and detected using ELISA. (e) Concentrations of α CD3HAC in the culture supernatants of HepG2 and SMMC-7721 cells infected with AdE1A- α CD3HAC at 50 MOI detected using ELISA every 24 h. All these results were expressed as the mean \pm SD for three separate experiments.

SMMC-7721 cells were also detected using dual-luciferase reporter assay (#E1910, Promega, USA) as described previously^{6,18}.

Isolation and culture of peripheral blood mononuclear cells

The blood of healthy donors was obtained from the Tianjin Blood Center. Peripheral blood mononuclear cells (PBMCs) were isolated using Ficoll solution (#LTS10771, TBD Science, China). The cells were maintained in RPMI 1640 plus 10% FBS and cultured in the presence of recombinant human interleukin-2 (IL-2, 100 U/mL; #202-IL-010, R&D) every other day.

Cell counting Kit-8 assay

The cell viability assay for the cytotoxicity of CRAd was performed using a cell counting kit-8 (CCK-8) kit (#CK04, Dojindo, Japan). The cells were seeded in a 96-well plate at the density of 1×10^4 cells/well and infected with different adenoviruses at 10, 50, or 100 multiplicities of infection (MOI). Then, the cell viabilities were evaluated every 24 h, from day 2 to day 4. The cells without infection were used as negative control. Each data point was averaged from three replicates of three separate experiments.

Establishment of PD-L1-overexpressing cell line

The sequences of human PD-L1 (Accession: NM_014143.4) and firefly luciferase were linked by the T2A sequence, and the linked sequence was inserted into the pCDH1-CMV-MSCEF1 α -Puro plasmid (#CD510B, SBI, USA) using *EcoRI* and *BamHI* restriction sites. The lentivirus was packaged as described previously¹⁹. SMMC-7721 cells were transduced with the lentivirus for 48 h and selected with 30 μ g/mL puromycin (#P8230; Beijing Solarbio Science & Technology, China) for 2 weeks. The new cell line was termed 7721-PD-L1.

Establishment of HepG2 with luciferase reporter

The sequence of firefly luciferase was inserted into the pCDH1-CMV-MSCEF1 α -Puro plasmid using *EcoRI* and *BamHI* restriction sites. The lentivirus was packaged and transfected into HepG2 cells as described previously. After selection using 30 μ g/mL puromycin, the stable cell line was established and termed HepG2-luc.

ELISA for α CD3HAC

HepG2 or SMMC-7721 cells were infected with different adenoviruses at 50 MOI for 48 h. The culture supernatants were collected, and the concentrations of α CD3HAC were measured using a His Tag ELISA Detection Kit (#L00436, GenScript, USA). Similarly, the concentrations of α CD3HAC in the supernatants of HepG2 or SMMC-7721 cells were measured using the same method every day after infection with AdE1A- α CD3HAC. The assays were performed in three replicates of three separate experiments.

α CD3HAC-binding detection

SMMC-7721 cells were infected with different adenoviruses for 96 h, following which the culture supernatants were collected to detect the binding of α CD3HAC to PD-L1 on 7721-PD-L1 cells by flow cytometry. For direct-binding assay, 1×10^5 cells were suspended in 100 μ L of the collected supernatant and mixed with 5 μ L of allophycocyanin (APC)-His tag antibody (#362605, Biolegend, USA). The cells without any supernatant were used as negative control, whereas the cells with APC-human PD-L1 antibody (#374514, Biolegend, USA) were used as positive control. After culturing at room temperature for 30 min, the cells were detected using flow cytometry (FACS). For the competition assay, 5 μ L of the APC-human PD-L1 antibody was added to the 7721-PD-L1 suspension of the collected supernatant. The cells with APC-isotype control (#982108, Biolegend, USA) were used as negative control, whereas the cells with only APC-human PD-L1 antibody were used as positive control. FACS was performed after culturing. The binding to CD3 was manipulated as earlier except for replacing the APC-human PD-L1 antibody with the APC-human CD3 antibody (#300312, Biolegend, USA).

Surface plasmon resonance assay

The α CD3HAC protein was expressed and purified as previously described¹⁴. And then the association and dissociation kinetics was detected by Biacore 8K (Cytiva, USA). Human recombinant CD3D & CD3E heterodimer protein and PD-L1 protein (#CT038-H2508H and #10084-H08H, Sino Biological, China) were immobilized via amine groups on the surface of the sensor chip CM5 (#BR100530, Cytiva, USA).

Cytotoxicity and activation of T cells

The culture supernatants of SMMC-7721 cells infected with different adenoviruses were still used in the following experiments. 7721-PD-L1 cells were seeded into 96-well plates (1×10^4 cells/well). The next day, PBMCs pretreated with IL-2 for 72 h were added at the effector: target (E:T) ratios of 5:1. Then, 100 μ L of the supernatant was added simultaneously. The specific cytotoxicity toward 7721-PD-L1 cells was measured by the lactate dehydrogenase assay 16 h later using a CytoTox 96 nonradioactive cytotoxicity kit (#G1780, Promega, USA) following the manufacturer's protocols. Then, the cells and the culture supernatant of every well were separated. The cells were stained with the APC-human CD3 antibody (#300312, Biolegend, USA) and the phycoerythrin (PE)-human CD69 antibody (#310906, Biolegend, USA) for 30 min at room temperature and measured using FACS to detect activated T cells. The levels of interleukin-2 (IL-2), interferon- γ (IFN- γ), and tumor necrosis factor- α (TNF- α) in the supernatants were measured using the corresponding ELISA kits (D2050, DIF50C, and DTA00D, R&D, USA).

Jurkat apoptosis assay

7721-PD-L1 and Jurkat cells were co-cultured in the supernatants collected previously at the ratio of 10:1 for 24 h. Then,

the cells were separated and stained with the APC-human CD3 antibody (#300312, Biolegend, USA) and fluorescein isothiocyanate (FITC) – Annexin V (#556547, BD, USA). The apoptosis of Jurkat cells was measured using FACS.

Adenovirus package in hepatic differentiated HUMSCs

HUMSCs were induced to undergo hepatic differentiation for 10 days and then infected with different adenoviruses at 500 MOI. The infected HUMSCs were separated at the indicated time point, and the copy numbers of viral DNA in these cells were measured by real-time polymerase-chain reaction (PCR) as described previously¹⁸. The HUMSCs collected 48 h after infection with AdE1A or AdE1A- α CD3HAC were observed using an electron microscope to find the adenovirus particles in the cells. Simultaneously, 50 μ L of the supernatant removed from the hepatic differentiated HUMSCs infected with different adenoviruses was co-cultured with HepG2 in 96-well plates at a density of 2500 cells/well. After 2 days, the HepG2 cells were observed under a fluorescence microscope to confirm the presence of adenovirus particles in the supernatants.

Transwell migration assay

HUMSCs were infected with the indicated adenovirus at 500 MOI for 48 h and plated at a density of 2×10^4 in the top chamber with 200 μ L of serum-free medium. The method was performed as described previously⁶.

Orthotopic hepatocarcinoma model

The orthotopic hepatocarcinoma model was established with HepG2-luc or 7721-PD-L1 cell line on BALB/c athymic nude mice as previously described⁶. For the AFP heterogeneous hepatocarcinoma model, HepG2 and 7721-PD-L1 cells were mixed at the ratio of 3:1, following which 2×10^7 cells were injected subcutaneously into the right anterior flank of mice. Subsequently, the same operation was performed as in the case of the orthotopic model.

Treatment of the orthotopic hepatocarcinoma model

After 10 days of orthotopic tumor inoculation, the mice were randomized into three to five groups (five mice for each group) according to the requirements. After infection with the indicated adenovirus at 500 MOI for 48 h, the HUMSCs were injected into each mouse (iv, 1×10^6 cells) on the first and fourth days. Then, PBMCs were injected (iv, 6×10^6 cells/mouse) on the seventh and tenth days. *In vivo*, the luciferase signal was monitored using Xenogen In Vivo Imaging System (IVIS) at the indicated time points. The body weight was recorded twice a week after the HUMSC injection. On the 18th day after treatment, the mice were sacrificed and the serum levels of alanine aminotransferase (ALT) and aspartate transaminase (AST) were assessed using detection kits (#C009-2-1 and #C010-2-1, Nanjing Jiancheng Bioengineering Institute, China). At the same time, the tissues of tumor and some extrahepatic organs, including the lung, kidney, and spleen, were removed from model mice. The total

RNA of tumor tissue was extracted using TRIzol reagent (#15596026, Invitrogen, USA), and the quantitative RT-PCR was performed to detect the expression of the PD-L1 gene as described previously¹⁹. The extrahepatic organs were fixed in 4% paraformaldehyde (PFA), embedded in paraffin, sectioned and stained with hematoxylin and eosin.

Immunofluorescence

The tumor tissues of orthotopic hepatocarcinoma models treated with adenovirus-armed HUMSCs for 4 days were cut into paraffin-embedded sections for immunofluorescence to explore the adenovirus delivery by HUMSCs. The sections were stained with mouse anti-Hexon primary antibody (#GTX36896, GeneTex, USA) and AF488-conjugated goat anti-mouse secondary antibody (#ab150113, Abcam, UK) to detect the adenovirus hexon protein. Meanwhile, rabbit anti-human CD90 primary antibody (#ab226123, Abcam, UK) and AF647-conjugated goat anti-rabbit secondary antibody (#ab150079, Abcam, UK) were used to indicate HUMSCs. The nuclei were stained with 4',6-diamidino-2-phenylindole (DAPI; #D9564, Sigma, USA). The images were captured using a two-photon laser scanning confocal microscope (FV1200 MPE, Olympus, Japan). Similarly, the tumor tissues of model mice treated with MSC.Ad and PBMC for 16 days were cut into paraffin-embedded sections and then stained with mouse anti-Hexon primary antibody, AF488-conjugated goat anti-mouse secondary antibody, rabbit anti-His tag primary antibody (#ab213204, Abcam, UK), and AF647-conjugated goat anti-rabbit secondary antibody to indicate hexon and α CD3HAC.

FACS for T cells in tumors

After the model mice were treated with MSC.Ad + PBMC for 16 days, the tumors were cut into approximately 1-mm³ pieces and digested with 0.05 mg/mL of type-IV collagenase (#C5138, Sigma, USA), hyaluronidase (#H3506, Sigma, USA), and DNase I (D5025, Sigma, USA) at 37°C for 60 min. Single cells were obtained by grinding and filtering through a 70- μ m strainer. Subsequently, mononuclear cells were obtained by density gradient centrifugation using 40% and 80% Percoll (#17-0891-09, GE, USA). The cells were stained with APC-human CD3 antibody and PE-human CD69 antibody. FACS was used to detect the activated T cells.

Co-culture and killing assay

Firstly, HepG2 cells were infected with different adenoviruses at 50 MOI for 24 h. Then, the infected HepG2 cells (2×10^4 cells/well) were seeded in the upper of the 24-well cell culture insert with 0.4- μ m pore filters (#353095, BD Falcon, USA), and 7721-PD-L1 cells (5×10^4 cells/well) were seeded in the lower. After co-culture for 48 h, the cell culture inserted with infected HepG2 cells was removed, and PBMCs (1×10^6 cells/well) were

added into and co-cultured with the 7721-PD-L1 cells for 24 h. Finally, the culture medium and suspended cells were all removed, and 500 μ L/well of D-luciferin (0.15 mg/mL; #P1043, Promega, USA) was added. Bioluminescence imaging was performed immediately using the Xenogen IVIS.

Statistical analysis

Data are represented as mean \pm SD. Significance was assayed by independent-sample *t* test, ANOVA and Tukey's test. A *P* value <0.05 indicated a statistically significant difference, whereas a *P* value <0.01 indicated a highly statistically significant difference.

Results

Functional identification of the CRAd loaded with α CD3HAC

The CRADs were constructed as shown in Figure 1a. One of them, designated as AdE1A, was used in the old targeting system. AdE1A- α CD3HAC was the improved one with the α CD3HAC expression cassette. Two HCC cell lines were selected as experimental objects with different AFP expression levels: HepG2 was the positive one, and SMMC-7721 was the negative one (Supp. 1A). Subsequently, the transcriptional activities of AFP and hTERT promoters were detected in these two cell lines. The activity of the AFP promoter was significantly higher in HepG2 cells than in SMMC-7721 cells, whereas the activity of the hTERT promoter was similar in both of them (Figure 1b). The survival of HepG2 cells was dramatically decreased by AdE1A and AdE1A- α CD3HAC in a dose-dependent manner because of the presence of E1A expression unit controlled by the AFP promoter and the miR-122 target sequence. The cell inhibitory effect of AdE1A- α CD3HAC was similar to that of AdE1A at the same MOI. However, the four adenoviruses, with or without the E1A expression unit, did not affect the survival of SMMC-7721 cells (Figure 1c).

Furthermore, the expression of α CD3HAC driven by the hTERT promoter was observed in HepG2 cells infected with Ad α CD3HAC or AdE1A- α CD3HAC (Supp. 1B). Likewise, the α CD3HACs secreted by HepG2 and SMMC-7721 cells infected with AdE1A or AdE1A- α CD3HAC were detectable in the culture supernatants (Figure 1d). Finally, variations in the α CD3HAC level were investigated in supernatants from 24 h to 96 h after infection with AdE1A- α CD3HAC. In the SMMC-7721 supernatant, the concentration of α CD3HAC followed a continuous upward trend for 96 h. However, in the HepG2 supernatant, the concentration of α CD3HAC did not increase remarkably at the point of 96 h after infection owing to the cell death resulting from the cytolytic effect of the CRAD (Figure 1e).

Function identification of α CD3HAC secreted from infected cells

An SMMC-7721 cell line overexpressing human PD-L1 (7721-PD-L1) was established firstly for determining the binding

activity of α CD3HAC to PD-L1. Then, the supernatants of SMMC-7721 infected with different adenoviruses for 96 h were collected for the following experiments. The direct binding and competition assays verified that the α CD3HACs in the supernatants of SMMC-7721 cells infected with Ad α CD3HAC or AdE1A- α CD3HAC could bind to 7721-PD-L1 and compete with the purchased PD-L1 antibody (Figure 2a,b). Similarly, α CD3HAC in the supernatant could also bind to Jurkat, a CD3-positive cell line, and compete with the purchased CD3 antibody (Figure 2c,d). The competitive ability of α CD3HAC to PD-L1 was less remarkable than which to CD3, because the binding sites of α CD3HAC and the purchased antibody were different on PD-L1, but the same on CD3. Furthermore, the affinity constants of α CD3HAC binding to CD3 and PD-L1 were confirmed by Biacore assay and the KD values were 1.15×10^{-10} and 3.00×10^{-10} respectively (Figure 2e,f).

After 7721-PD-L1 (target cells) and PBMCs (effect cells) were co-cultured with the medium containing the indicated supernatants separately for 24 h, more than 60% of target cells were eliminated by effector cells in the medium containing α CD3HAC (Figure 2g). Furthermore, we observed the interaction between the target and effect cells mediated by α CD3HAC using living cells workstation (Supp. 2). Also, the proportions of CD69-positive (activated) T cells were increased to about 90% by α CD3HAC (Figures. 2h, Supp. 3). As the products of activated T cells, the levels of IL-2, IFN- γ , and TNF- α in the co-culture medium containing α CD3HAC also remarkably increased (Figure 2i-k). Under this condition, the T cell proliferation mediated by α CD3HAC was detectable (Supp. 4). As the negative controls, the cytolytic effect and the activation of T cells and the increases of IL-2, IFN- γ , and TNF- α mediated by α CD3HAC on SMMC-7721 and HL-7702 (a human normal liver cell line) were all not observed (Supp. 5). PD-L1 on tumor cells has the function of inducing T cell apoptosis by interacting with PD-1. Therefore, the apoptosis of Jurkat (PD-1-positive) co-culturing with 7721-PD-L1 cells and the collected supernatants of infected SMMC-7721 were detected. The result showed that α CD3HAC inhibited the PD-L1 induced apoptosis (Figure 2l, Supp. 6).

Package and delivery of adenovirus by HUMSCs

After induced hepatic differentiation for 10 days *in vitro*, HUMSCs were loaded with different adenoviruses. These HUMSCs were collected every day to measure the copies of viral DNA in them for 3 days. The curves in Figure 3a demonstrate that the content of adenovirus in differentiated HUMSCs peaked at the point of 48 h after infection with AdE1A or AdE1A- α CD3HAC, but no viral DNA was detected in the HUMSCs infected with other adenoviruses. Under the electron microscope, adenovirus particles were discovered in differentiated HUMSCs infected with AdE1A or AdE1A- α CD3HAC (Figure 3b). The supernatants of differentiated HUMSCs loaded with the adenoviruses were added onto HepG2 cells to verify that the packaged adenovirus could be released from the HUMSCs. After 2 days, HepG2 cells with the supernatant from MSC.AdE1A or MSC.AdE1A- α CD3HAC showed clustered green fluorescence because the corresponding adenoviruses

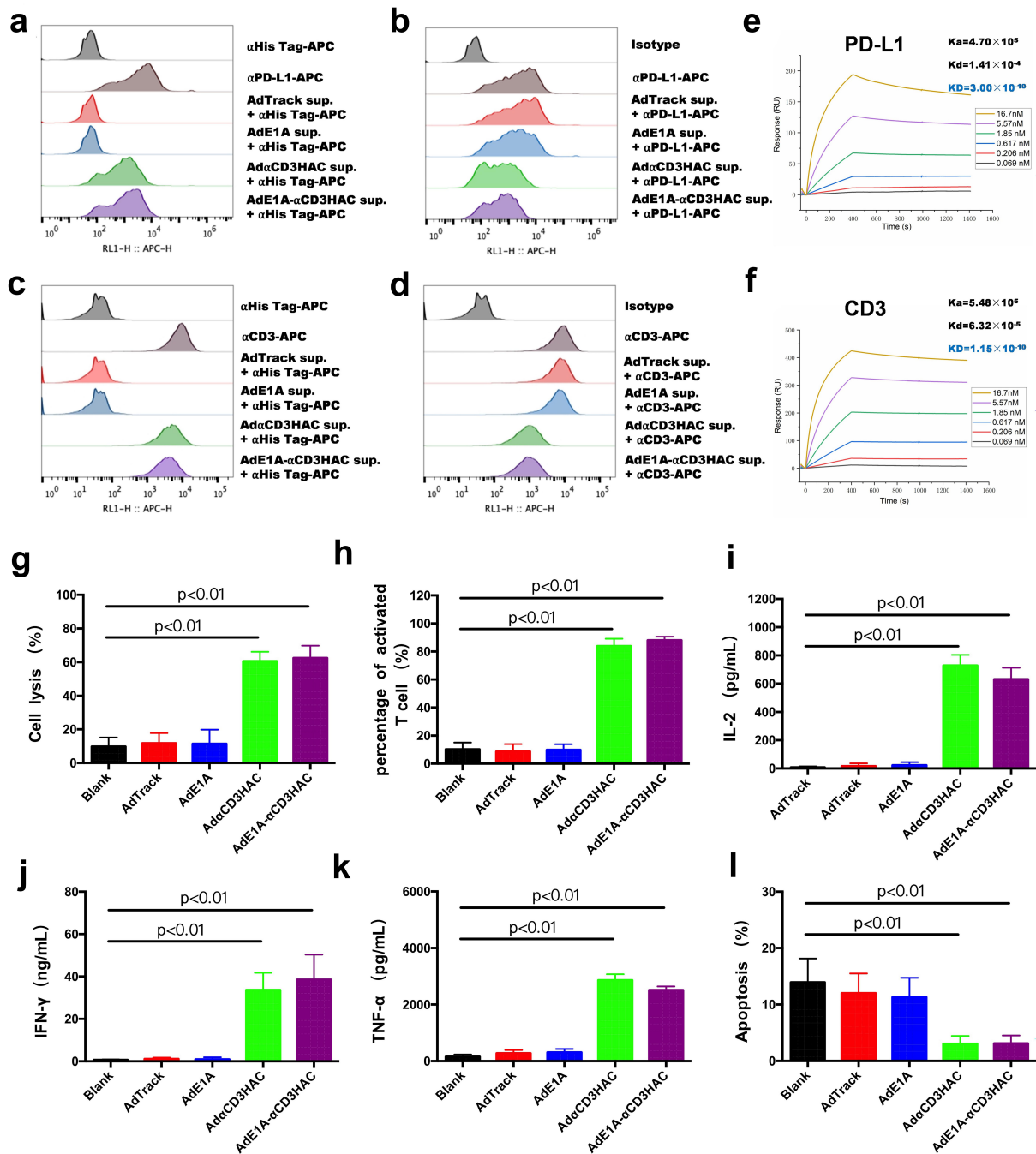


Figure 2. Identification of α CD3HAC in the culture supernatants. The culture supernatants of SMMC-7721 cells infected with different adenoviruses at 50 MOI for 96 h were collected for the direct-binding assay and competitive-binding assay (A-D). (a) Direct binding activities of the culture supernatants to PD-L1 detected by FACS on 7721-PD-L1 cells. The APC-human PD-L1 antibody was used as positive control, and the APC-His tag antibody was used as the secondary antibody. (b) Competitive binding activities of culture supernatants with the purchased APC-human PD-L1 antibody detected on 7721-PD-L1 cells using FACS. (c) Direct binding activities of culture supernatants to human CD3 detected using FACS on Jurkat cells. The APC-human CD3 antibody was used as positive control, and the APC-His tag antibody was used as the secondary antibody. (d) Competitive binding activities of culture supernatants with the purchased APC-human CD3 antibody detected on Jurkat cells using FACS. (e,f) Association and dissociation kinetics detected by Biacore assay. Human recombinant CD3D & CD3E heterodimer protein and PD-L1 protein were immobilized on the sensor chip CM5. Corresponding sensorgrams collected by Biacore 8K with analyte concentrations from 0.069 to 16.7 nM (color gradient) for the purified α CD3HAC. (g) PBMCs and 7721-PD-L1 cells were co-cultured in the collected supernatants of the infected SMMC-7721 cells at the ratio of 5:1 for 16 h, and the specific cytotoxicity toward 7721-PD-L1 cells was measured by lactate dehydrogenase assay using the CytoTox 96 nonradioactive cytotoxicity kit. (h) Cell component in the co-culture system was collected and stained with the APC-human CD3 antibody and the PE-human CD69 antibody for detecting activated T cells using FACS. (i-k) Supernatants of the co-culture system were measured using ELISA for the concentrations of IL-2, IFN- γ , and TNF- α . (l) 7721-PD-L1 and Jurkat cells were co-cultured in the collected supernatants of infected SMMC-7721 cells at the ratio of 10:1 for 24 h. Then, the cells were separated and stained with the APC-human CD3 antibody and FITC - Annexin V. The apoptosis of Jurkat cells was measured using FACS. The results in (G - L) represent the mean \pm SD for three separate experiments.

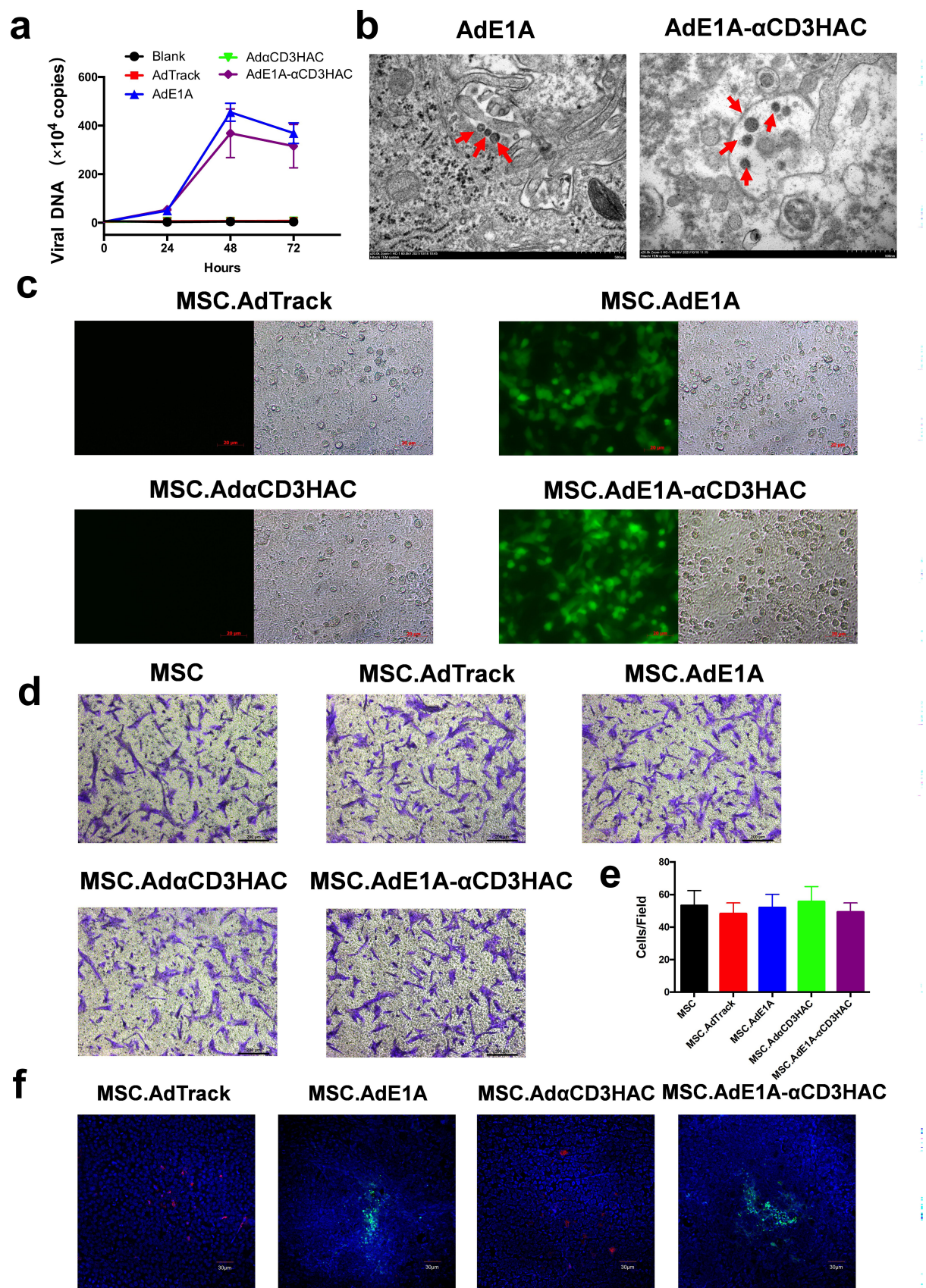


Figure 3. Package and delivery of adenovirus by HUMSCs. (a) DNA copy numbers of adenovirus in the hepatic differentiated HUMSCs detected by real-time PCR at the indicated time point after infection with different adenoviruses. This result represented the mean \pm SD for three separate experiments. (b) Representative images of adenovirus particles in the hepatic differentiated HUMSCs infected with AdE1A or AdE1A- α CD3HAC observed under the electron microscope. Adenovirus particles are indicated by red arrows. Scale bar, 500 nm. (c) Representative fluorescence microscopic images of HepG2 cells treated with the culture supernatants of the hepatic differentiated HUMSCs infected with different adenoviruses. The HepG2 cells showed green fluorescence due to the supernatant containing adenovirus particles. Scale bar, 20 μ m. (d, e) Transwell migration assay. Representative images of migrated HUMSCs stained with crystal violet after infection with different adenoviruses for 2 days

were released into supernatants from differentiated HUMSCs and propagated in the AFP-positive cells after infecting them, but the cells with the supernatant from MSC.AdTrack or MSC.Ad α CD3HAC did not (Figure 3c).

On the contrary, the Transwell assay showed that the migration capability of HUMSCs was not affected by loading with adenovirus (Figure 3d,e). MSC.ads were intravenously injected into the orthotopic hepatocarcinoma model mice to investigate the delivery of adenovirus by HUMSCs *in vivo*. The tumor tissues were removed and observed under a confocal microscope 4 days later. The tissues from mice treated with MSC.AdTrack or MSC.Ad α CD3HAC showed scattered HUMSCs marked by the CD90-antibody (red). However, HUMSCs disappeared in the tumor tissues of mice treated with MSC.AdE1A or MSC.AdE1A- α CD3HAC and were replaced by clustered adenoviruses stained with the hexon antibody (green) (Figure 3f). It indicated that the MSC.Ads could home into tumor tissues, and the HUMSCs loaded with adenovirus containing the E1A expression cassette were lysed and releasing the adenovirus.

Inhibitory effect against the orthotopic liver xenograft tumor

In order to explore the tumor-inhibitory effect of the new improved targeting system, orthotopic hepatocarcinoma model mice were established using HepG2-luc and administered with the MSC.Ads and PBMCs as shown in Figure 4a. After 8 days of treatment, the tumors were inhibited significantly by MSC.AdE1A or MSC.AdE1A- α CD3HAC, but with no remarkable difference between these two treatment groups. Subsequently, on the 16th day after treatment, the tumors of the MSC.AdE1A + PBMC or MSC.AdE1A- α CD3HAC + PBMC groups were still smaller than those of the other groups. From the 8th day to the 16th day, the treatment with MSC.AdE1A- α CD3HAC + PBMC achieved a better tumor-inhibitory effect than MSC.AdE1A + PBMC because of the α CD3HAC-mediated antitumor function of PBMCs (Figures 4b,c, Supp. 7, 8). Subsequently, the TUNEL assay was performed on the tumor tissue sections. From the images of confocal microscope, we observed a mass of dead cells in the tumor treated by MSC.AdE1A + PBMC or MSC.AdE1A- α CD3HAC + PBMC (Supp. 9).

ALT and AST levels in serum were detected to evaluate liver injuries in these model mice under different therapeutic strategies. As shown in Figure 4d, the levels of ALT and AST declined after treatment with MSC.AdE1A + PBMC or MSC.AdE1A- α CD3HAC + PBMC; the ALT levels were remarkably different between these two groups but the AST levels were not. Additionally, no marked difference was found in weight change and pathologic features of extrahepatic organs among all treatment groups (Figure 4e,f).

Adenovirus and INF- γ could promote PD-L1 expression so that the PD-L1 level in tumors was measured using quantitative PCR. As expected, the levels of PD-L1 in the tumors in the MSC.AdE1A + PBMC and MSC.AdE1A- α CD3HAC + PBMC treatment groups were elevated obviously. Although the PD-L1-positive cells were the target of T cells mediated by α CD3HAC, no significant difference was found in the PD-L1 expression level between these two groups (Figure 4g).

Expression of α CD3HAC and activation of T cells in tumor tissues

Confocal microscopy was performed to verify the expression of α CD3HAC in tumor tissues. Adenovirus hexon protein (green) and α CD3HAC (red) were both found on the tumor tissue sections of the MSC.AdE1A- α CD3HAC + PBMC treatment group, and their distributions were similar. Only hexon, but no α CD3HAC, was shown on the sections of the MSC.AdE1A + PBMC group; neither hexon nor α CD3HAC was found in the tumors of the other groups (Figure 5a). The infection and proliferation of adenoviruses in tumors could promote T lymphocyte infiltration; α CD3HAC could maintain their survival by activating them directly and blocking PD-L1 to prevent inactivation. Therefore, lymphocytes in tumors were isolated and the proportion of activated T cells was measured using FACS. Few CD3-positive T cells were found in the tumors of the MSC.AdTrack + PBMC and MSC.Ad α CD3HAC + PBMC groups (Supp. 10). However, the infiltration of T cells increased significantly in the tumors of the MSC.AdE1A + PBMC and MSC.AdE1A- α CD3HAC + PBMC groups (Figure 5b). Moreover, the proportions of not only total T cells but also activated T cells in the tumors of the MSC.Ad α CD3HAC + PBMC group were higher than those of the MSC.AdE1A + PBMC group (Figure 5c,d, Supp. 11).

Inhibitory effect on the AFP heterogeneous hepatocarcinoma model

Previously, it was identified that both AdE1A and AdE1A- α CD3HAC could not cause SMMC-7721 cell lysis *in vitro* (Figure 1c). In this study, the treatment effects of MSC.AdE1A + PBMC and MSC.AdE1A- α CD3HAC + PBMC on 7721-PD-L1 orthotopic liver xenograft model mice were further considered. Although α CD3HAC could be released by 7721-PD-L1 infected with AdE1A- α CD3HAC, the treatment of MSC.AdE1A- α CD3HAC + PBMC, similar to MSC.AdE1A + PBMC, did not inhibit the tumor growth (Figure 6a,b, Supp. 12A). It was speculated that α CD3HAC was not sufficient to evoke the antitumor effect of T lymphocytes in the unitary AFP-negative tumor model. If tumor tissues contained both AFP-positive and AFP-negative cells, the amounts of α CD3HAC were supported by the replication of AdE1A- α CD3HAC in AFP-positive cells to facilitate the clearance of

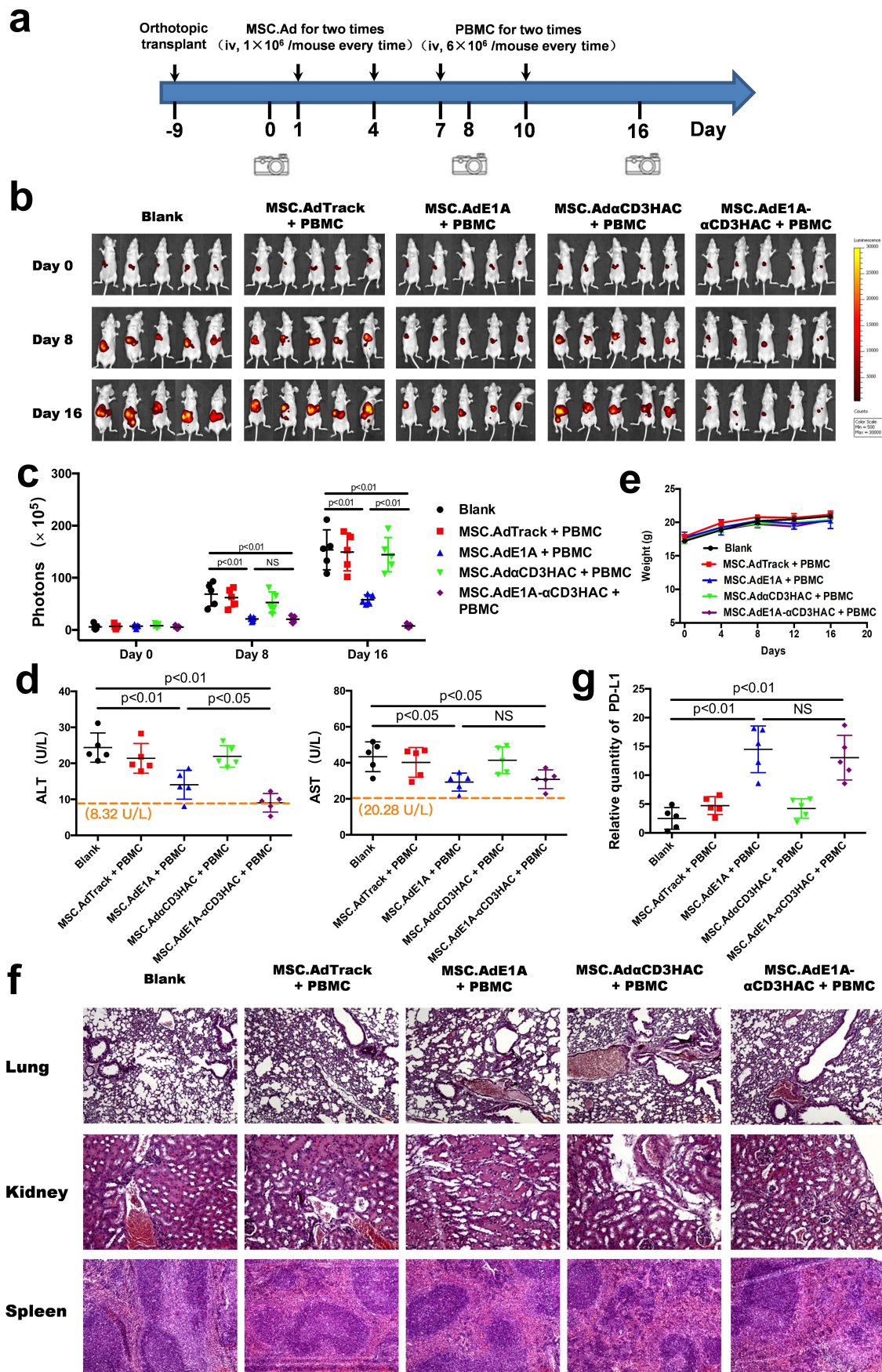


Figure 4. Tumor suppression of MSC.AdE1A- α CD3HAC in combination with PBMCs against liver orthotopic transplantation tumors. (a) Design and timeline for therapeutic strategy. (b) IVIS images of HepG2-Luc cells were shown for all treatment groups ($n = 5$ per group) at the indicated time point. (c) Quantification of luciferase signals on all model mice at the indicated time point. (d) Levels of ALT and AST in the serum of all model mice after treatment for 16 days. Orange dotted lines indicate the mean values of ALT and AST concentrations in five healthy BALB/c athymic nude mice (without tumor). (e) Average body weight of five groups ($n = 5$ per group) of HepG2 orthotopic transplantation model mice during treatment. (f) Representative images of sectioned organs (lung, kidney, and spleen) from the model mice in different treatment groups after hematoxylin and eosin staining. (g) Relative level of PD-L1 expressed in the tumor tissues of all treatment groups detected by real-time PCR.

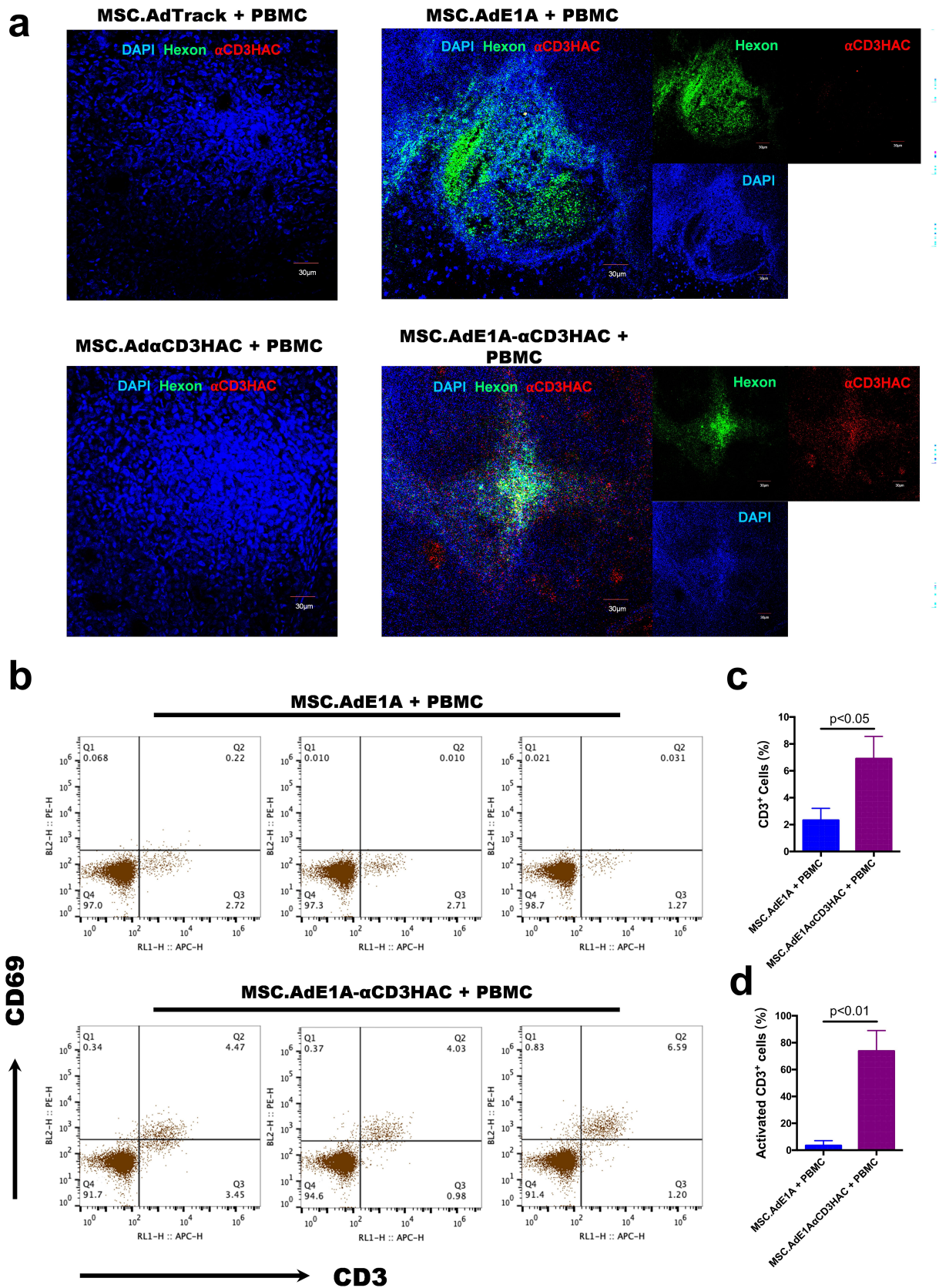


Figure 5. Expression of α CD3HAC and activation of T cells in tumor tissues. (a) Representative confocal microscope images for the tumor tissues in each treatment group on the 16th day. Green (anti-hexon protein) indicates adenovirus, red (anti-His tag) indicates α CD3HAC, and blue (DAPI) indicates nuclei. Scale bar, 30 μ m. (b) Lymphocytes isolated from the tumor tissues of model mice in the MSC.AdE1A + PBMCs and MSC.AdE1A- α CD3HAC + PBMCs treatment groups ($n = 3$ per group) were stained with APC-human CD3 antibody and PE-human CD69 antibody and analyzed using FACS. (c) Statistical graph of the FACS assay on the percentage of T cells in tumors. (d) Statistical graph of the FACS assay on the percentage of the activated T cells (CD69⁺CD3⁺/CD3⁺).

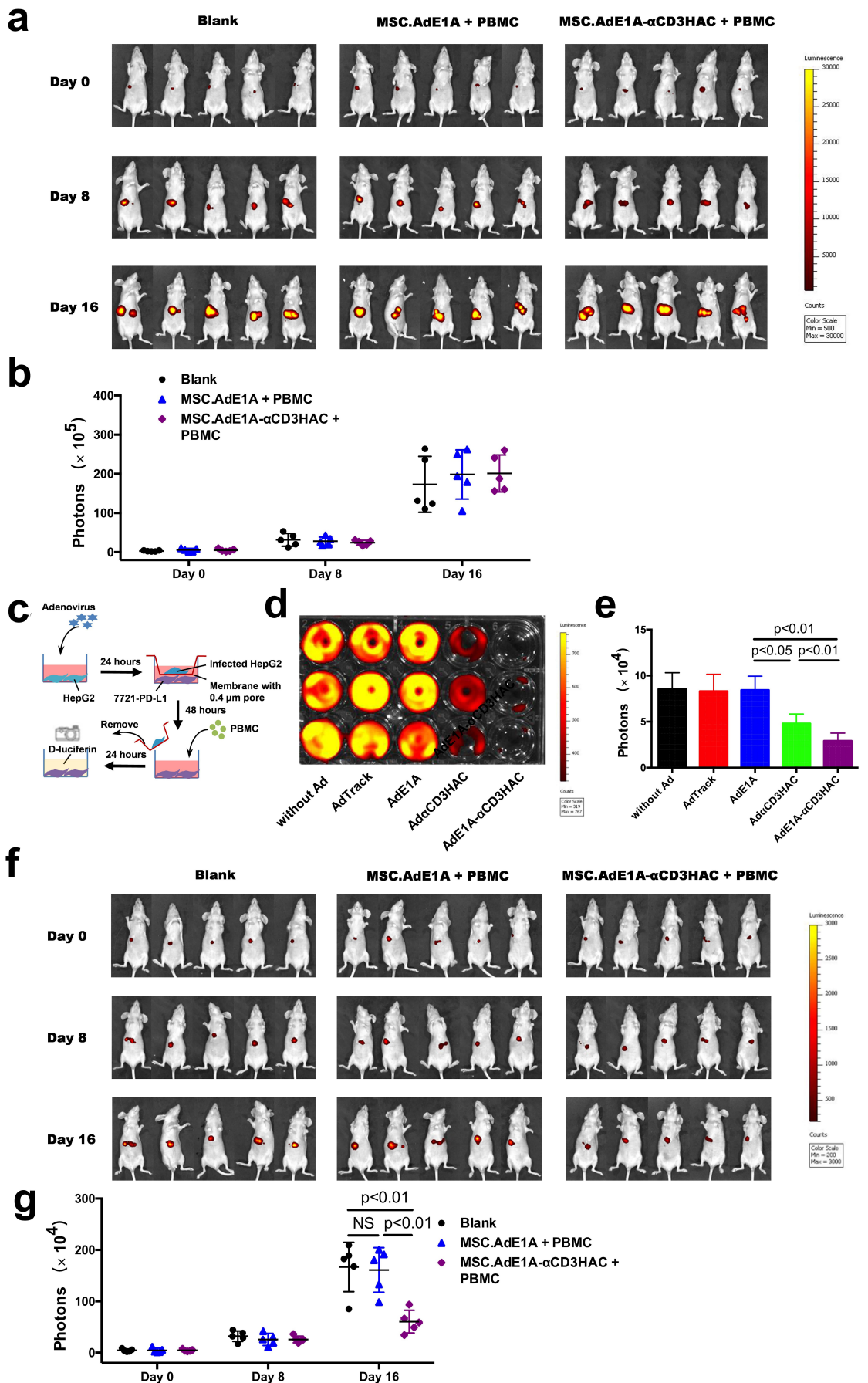


Figure 6. Inhibitory effect on the AFP heterogeneous hepatocarcinoma model. (a) IVIS images of 7721-PD-L1 cells were shown for all treatment groups ($n = 5$ per group) on 7721-PD-L1 orthotopic transplantation model mice at the indicated time point. (b) Quantification of luciferase signals on all model mice at the indicated time point.

the AFP-negative cells. A co-culture experiment was performed to test this assumption, as shown in Figure 6c. The result demonstrated that the killing effect against 7721-PD-L1 mediated by HepG2 infected with AdE1A- α CD3HAC was more significant than that mediated by HepG2 infected with Ad α CD3HAC (Figure 6d,e). This was because the released adenovirus spread into the lower chamber through the membrane with 0.4- μ m pores and infected the 7721-PD-L1, resulting in a higher concentration of α CD3HAC remaining in the supernatant. Subsequently, the treatment of the AFP heterogeneous tumor model with MSC.AdE1A- α CD3HAC + PBMC was evaluated. The luciferase reporter signal of 7721-PD-L1 remarkably decreased in the group treated with MSC.AdE1A- α CD3HAC + PBMC compared with the untreated group and the group treated with MSC.AdE1A+PBMC (Figure 6f,g, Supp. 12B). This result indicated that MSC.AdE1A- α CD3HAC + PBMC could be used to overcome the problem resulting from AFP heterogeneity.

Discussion


Since we found that the AFP promoter was activated during the hepatic differentiation of HUMSCs, the HUMSCs were used as the *in vivo* delivery vehicle of CRAds or therapeutic proteins controlled by the AFP promoter against HCC^{6,18,20,21}. For the specific replication of the CRAd in hepatoma cells, the AFP promoter was an important regulator; and the miR-122 target sequence was another regulator for further reducing the side effects on normal hepatocytes⁶. Although the CRAd delivered by HUMSCs had a better antitumor effect and safety, it still needed improvement for two reasons: (1) The tumor inhibition rate was unsatisfactory so that the combination with other antitumor strategies was necessary. (2) The intratumoral heterogeneous expression of AFP was an important feature of HCC^{22,23}, and hence the selectivity of the CRAd only to AFP-positive cells resulted in failure to eliminate tumors completely.

Nowadays, many BiTEs have been armed on CRAds to exert a synergistic antitumor effect^{8,9,24}. In this study, we established a novel CRAd (AdE1A- α CD3HAC) with a PD-L1 targeting BiTE (α CD3HAC), which was applied in treating TNBC previously¹⁴. In the sequence of α CD3HAC, the part of anti-CD3 scFv was cloned from the variable region of an immunoglobulin G antibody (HIT3a), and the part of HAC was a mutant of PD-1 ectodomain with high affinity to PD-L1²⁵. The expression of α CD3HAC was under the control of the hTERT promoter, a known tumor-specific promoter, which guaranteed the release of α CD3HAC from both AFP-positive cells and AFP-negative cells after infection. After a series of identification experiments including selective killing activity of CRAd, release and binding activity of α CD3HAC, and α CD3HAC-mediated T cell activation, it was confirmed that the characteristics of AdE1A- α CD3HAC were as expected.

It was validated that AdE1A could be delivered and packaged by HUMSCs in a previous study⁶. The *in vitro* experiments showed that AdE1A- α CD3HAC was similar to AdE1A in terms of adenovirus package and HUMSC migration when loaded on HUMSCs. On the orthotopic xenograft model mice, CRAds were observed in tumor tissues of the MSC.AdE1A and MSC.AdE1A- α CD3HAC treatment groups at the appropriate time point. It indicated that, like AdE1A, AdE1A- α CD3HAC was delivered and released by HUMSCs *in vivo*.

The expression of PD-L1 was high in HCC and increased after stimulation by virus and IFN- γ ²⁶⁻³⁰. The existence of large amounts of PD-L1 in tumors was not beneficial to the survival of effector lymphocytes. The reason of choosing α CD3HAC to enhance the antitumor effect was that it not only blocked PD-L1 to cause T cell survival but also activated T cells for proliferation and specific killing. The detection of lymphocytes isolated from tumor tissues of orthotopic xenograft model mice using FACS verified that α CD3HAC increased the proportion of intratumoral T cells and made them active. Therefore, the sequential therapy of MSC.AdE1A- α CD3HAC + PBMC had a better antitumor effect than MSC.AdE1A + PBMC on orthotopic hepatocarcinoma models. Before PBMCs came into play, MSC.AdE1A- α CD3HAC and MSC.AdE1A achieved similar inhibition rates. Along with the participation of PBMCs, the function of α CD3HAC was exhibited, which resulted in a further increase in the tumor inhibition rate of the MSC.Ad α CD3HAC + PBMC group. After treatment, we discovered that PD-L1 levels in tumor tissues of the MSC.AdE1A- α CD3HAC + PBMC and MSC.AdE1A + PBMC treatment groups were remarkably higher than those of the other groups. Although α CD3HAC mediated the specific lysis of PD-L1-positive cells, the total PD-L1 level in tumor tissues of the MSC.AdE1A- α CD3HAC + PBMC treatment group did not decline significantly. This result hinted that the function of α CD3HAC did not disappear in a short time when the model mice were treated with MSC.Ad α CD3HAC + PBMC. Additionally, it also had been found that the intratumoral T cells were significantly increased in the both MSC.AdE1A- α CD3HAC + PBMC and MSC.AdE1A + PBMC treatment group. I think there are two reasons for it: (1) the physical barrier is broken by the cytolytic effect of the CRAd; (2) under the stimulation of adenovirus, some chemokines are released from the tumor tissue.

Many mechanisms were designed in the new system to avoid side effects: (1) The homing and hepatic differentiation of HUMSC controlled the release of CRAds only in the tumor tissues. (2) The AFP promoter and miR-122 target sequence ensured the selectivity of tumor cells. (3) The hTERT promoter was active in tumor cells but inactive in HUMSCs¹⁸ so that the distribution of α CD3HAC was limited to the local tumor site. According to the aforementioned designs, the treatment with MSC.AdE1A- α CD3HAC + PBMC did not affect the body weight and extrahepatic organs. As the biomarkers of liver

(c) Schematic representation of the co-culture and killing assay () indicated monitoring of the luciferase signal using the Xenogen IVIS imaging system. (d) Representative IVIS image of residual 7721-PD-L1 cells in the co-culture and killing assay. (e) Quantification of luciferase signals of the residual 7721-PD-L1 cells. (f) IVIS images of 7721-PD-L1 cells were shown for all treatment groups ($n = 5$ per group) on AFP heterogeneous hepatocarcinoma model mice at the indicated time point. (g) Quantification of luciferase signals on the AFP heterogeneous hepatocarcinoma model mice at the indicated time point.

injury, the serum ALT and AST levels declined in the model mice of the MSC.AdE1A- α CD3HAC + PBMC and MSC.AdE1A + PBMC treatment groups. Compared with the MSC.AdE1A + PBMC group, the MSC.AdE1A- α CD3HAC + PBMC group showed lower levels of ALT.

The immunotherapy against HCC faced many problems similar to other solid tumors, such as effective and safe targeting, infiltration and survival of lymphocytes, tumor heterogeneity, and immunosuppressive microenvironment^{31,32}. Based on the aforementioned findings, it was concluded that the new targeting system solved the first two problems to a large extent. In the old system, the recognition of tumor cells mainly depended on the AFP promoter, and therefore the heterogeneous expression of AFP in tumors limited its antitumor effect. α CD3HAC at the local tumor site could re-target tumor cells by PD-L1, so that the treatment with MSC.Ad α CD3HAC + PBMC showed obvious killing capacity against AFP-negative tumor cells on AFP heterogeneous model mice. Theoretically, several mechanisms by which AdE1A- α CD3HAC overcame the problem of tumor microenvironment were available^{32–34}. However, the tumor xenograft models in this study were established using BALB/c athymic nude mice, and hence the influence of α CD3HAC on the tumor microenvironment was not exhibited sufficiently. Therefore, the change in the tumor microenvironment caused by CRAd and α CD3HAC on humanized mice should be further explored in future studies.

Conclusions

A BiTE, α CD3HAC, driven by the hTERT promoter, was loaded on the CRAd of the old HCC-targeting system to overcome the limitation caused by the selectivity of the AFP-positive cells and strengthen the antitumor effect. The new system exhibited a better antitumor effect with no more damage to extrahepatic organs and less liver injury, compared with the old one. The α CD3HAC released from the AFP-positive cells re-targeted the PD-L1-positive cells to facilitate the elimination of the AFP-negative cells in the AFP heterogeneous tumor model. Taken together, the new system provided a more effective and safer strategy against HCC.

Abbreviations

HCC: Hepatocellular carcinoma; CRAd: Conditionally replicative adenovirus; HUMSC: Human umbilical cord – derived mesenchymal stem cell; AFP: Alpha-fetoprotein; BiTE: Bispecific T cell engager; scFv: Single-chain variable fragment; PD-L1: Programmed death ligand 1; hTERT: Human telomerase reverse transcriptase; PCR: Polymerase chain reaction; ALT: Alanine aminotransferase; AST: Aspartate transaminase; IVIS: In Vivo Imaging System; MOI: Multiplicity of infection; ELISA: Enzyme-linked immune sorbent assay; PBMC: Peripheral blood mononuclear cell;

Authors' contributions

XY wrote the main manuscript and designed and performed all the experiments. YL constructed the adenoviruses, established the stable expression cell line, and participated in animal operation. YY prepared all figures, performed electron microscope assay, and participated in animal operation. WT contributed to H&E staining and confocal

microscopic imaging. YY and DF participated in the isolation of PBMCs and HUMSCs. RL assisted in FACS. XL performed Western blotting and luciferase assays. YX helped in ELISA. LY participated in cytotoxicity experiments. SY and DX were the corresponding authors; they participated in the design of the study and revised the manuscript. All authors read and approved the final manuscript.

Ethics approval and consent to participate

All animal studies were performed following the guidelines from the Animal Ethics Committee of the Tianjin NanKai Hospital.

Data Availability statement

The dataset supporting the conclusions of this study is included in the manuscript.

Disclosure statement

No potential conflict of interest was reported by the author(s).

Funding

This study was supported by the Tianjin Municipal Science and Technology Commission Grant (Grant No. 19JCZDJC33100); the National Natural Science Foundation of China (Grant Nos. 82003266 and 81830005); CAMS Innovation Fund for Medical Sciences (Grant No. 2021-I2M-1-041); Haihe Laboratory of Cell Ecosystem Innovation Fund (Grant No. HH22KYZX0032); Scientific Foundation of Tianjin Municipal Education Commission (Grant No. 2019KJ196).

References

- Dong Yang J, Hainaut P, Gores GJ, Amadou A, Plymoth A, Roberts LR. A global view of hepatocellular carcinoma: trends, risk, prevention and management. *Nat Rev Gastroenterol Hepatol.* 2019;16(10):589–604. doi:10.1038/s41575-019-0186-y.
- Greten TF, Walter Lai C, Guangfu L, Staveley-O'Carroll KF. Targeted and immune-based therapies for hepatocellular carcinoma. *Gastroenterology.* 2019;156(2):510–524. doi:10.1053/j.gastro.2018.09.051.
- Ruf B, Heinrich B, Greten TF. Immunobiology and immunotherapy of HCC: spotlight on innate and innate-like immune cells. *Cell Mol Immunol.* 2021 Jan;18(1):112–127. doi:10.1038/s41423-020-00572-w.
- Pinato DJ, Guerra N, Fessas P, Murphy R, Mineo T, Mauri FA, Mukherjee SK, Thursz M, Ngar Wong C, Sharma R, et al. Immune-based therapies for hepatocellular carcinoma. *Oncogene.* 2020;39(18):3620–3637. doi:10.1038/s41388-020-1249-9.
- Hafezi M, Lin M, Chia A, Chua A, Zi Zong H, Fam R, Tan D, Joey A, Pavesi A, Lee Krishnamoorthy T, et al. Immunosuppressive drug-resistant armored T-Cell receptor t cells for immune therapy of HCC in liver transplant patients. *Hepatology.* 2021;74(1):200–213. doi:10.1002/hep.31662.
- Yuan X, Zhang Q, Zhenzhen L, Zhang X, Bao S, Fan D, Yongxin R, Dong S, Zhang Y, Zhang Y, et al. Mesenchymal stem cells deliver and release conditionally replicative adenovirus depending on hepatic differentiation to eliminate hepatocellular carcinoma cells specifically. *Cancer Lett.* 2016;381(1):85–95. doi:10.1016/j.canlet.2016.07.019.
- Manuela Arnone C, Assunta Polito V, Mastronuzzi A, Carai A, Camassei Diomedi F, Antonucci L, Lisa Petrilli L, Vinci M, Ferrari F, Salviato E, et al. Francesca Del Bufalo. Oncolytic adenovirus and gene therapy with EphA2-BiTE for the treatment of pediatric high-grade gliomas. *J Immunother Cancer.* 2021;9(5):e001930. doi:10.1136/jitc-2020-001930.

8. Johannes PWH, Engeland CE. Oncolytic viruses encoding bispecific T cell engagers: a blueprint for emerging immunovirotherapies. *J Hematol Oncol.* 2021;14(1):63. doi:10.1186/s13045-021-01075-5.
9. Porter CE, Rosewell Shaw A, Jung Y, Yip T, Castro PD, Sandulache VC, Sikora A, Gottschalk S, Ittman MM, Brenner MK, et al. Oncolytic adenovirus armed with BiTE, Cytokine, and checkpoint inhibitor enables CAR T cells to control the growth of heterogeneous tumors. *Mol Ther.* 2020;28(5):1251–1262. doi:10.1016/j.ymthe.2020.02.016.
10. Zhou S, Liu M, Ren F, Meng X, Jinming Y. The landscape of bispecific T cell engager in cancer treatment. *Biomark Res.* 2021;9(1):38. doi:10.1186/s40364-021-00294-9.
11. Tedcastle A, Illingworth S, Brown A, Seymour LW, Fisher KD. Actin-resistant DNase I expression from oncolytic adenovirus enadenotucirev enhances its intratumoral spread and reduces tumor growth. *Mol Ther.* 2016;24(4):796–804. doi:10.1038/mt.2015.233.
12. Sheng Guo Z, Binfeng L, Guo Z, Giehl E, Feist M, Dai E, Liu W, Storkus WJ, Yukai H, Liu Z, et al. Vaccinia virus-mediated cancer immunotherapy: cancer vaccines and oncolytics. *J ImmunoTher Cancer.* 2019;7(1):6. doi:10.1186/s40425-018-0495-7.
13. Tian Y, Xie D, Yang L. Engineering strategies to enhance oncolytic viruses in cancer immunotherapy. *Signal Transduct Target Ther.* 2022;7(1):117. doi:10.1038/s41392-022-00951-x.
14. Yang Y, Zhang X, Lin F, Xiong M, Fan D, Yuan X, Yang L, Song Y, Zhang Y, Hao M, et al. Bispecific CD3-HAC carried by E1A-engineered mesenchymal stromal cells against metastatic breast cancer by blocking PD-L1 and activating T cells. *J Hematol Oncol.* 2019;12(1):46. doi:10.1186/s13045-019-0723-8.
15. Murai H, Kodama T, Maesaka K, Tange S, Motooka D, Suzuki Y, Shigematsu Y, Inamura K, Mise Y, Saiura A, et al. Hidetoshi Eguchi, Eiichi Morii, Tetsuo Takehara. Multiomics identifies the link between intratumor steatosis and the exhausted tumor immune microenvironment in hepatocellular carcinoma. *Hepatology.* 2022 May 14;77(1):77–91. doi:10.1002/hep.32573.
16. Rizzo A, Dalia Ricci A, Di Federico A, Frega G, Palloni A, Tavolari S, Brandi G. Predictive biomarkers for checkpoint inhibitor-based immunotherapy in hepatocellular carcinoma: where do we stand? *Front Oncol.* 2021;11:803133. doi:10.3389/fonc.2021.803133.
17. Zhang X, Yang Y, Zhang L, Yang L, Zhang Q, Fan D, Zhang Y, Zhang Y, Zhou Y, Xiong D. Mesenchymal stromal cells as vehicles of tetravalent bispecific Tandab (CD3/CD19) for the treatment of B cell lymphoma combined with IDO pathway inhibitor D-1-methyl-tryptophan. *J Hematol Oncol.* 2017;10(1):56. doi:10.1186/s13045-017-0397-z.
18. Zhenzhen L, Zhou Y, Zhang X, Zhang Q, Fan D, Zhang Y, Luo HR, Yuan X, Zongfang L, Xiong D. E1A-engineered human umbilical cord mesenchymal stem cells as carriers and amplifiers for adenovirus suppress hepatocarcinoma in mice. *Oncotarget.* 2016;7(32):51815–51828. doi:10.18632/oncotarget.10122.
19. Yuan X, Tian W, Hua Y, Lijuan H, Yang J, Xie J, Jiakai H, Wang F, Feng Wang. Rhein enhances the cytotoxicity of effector lymphocytes in colon cancer under hypoxic conditions. *Exp Ther Med.* 2018;16(6):5350–5358. doi:10.3892/etm.2018.6855.
20. Yan C, Yang M, Zhenzhen L, Shuangjing L, Xiao H, Fan D, Zhang Y, Wang J, Xiong D. Suppression of orthotopically implanted hepatocarcinoma in mice by umbilical cord-derived mesenchymal stem cells with sTRAIL gene expression driven by AFP promoter. *Biomaterials.* 2014;35(9):3035–3043. doi:10.1016/j.biomaterials.2013.12.037.
21. Zhang Q, Yuan X, Yang L, Zhenzhen L, Bao S, Zhang X, Yang Y, Fan D, Zhang Y, Chenxuan W, et al. Surface expression of anti-CD3scfv stimulates locoregional immunotherapy against hepatocellular carcinoma depending on the E1A-engineered human umbilical cord mesenchymal stem cells. *Int J Cancer.* 2017;141(7):1445–1457. doi:10.1002/ijc.30846.
22. Andreas Ridder D, Weinmann A, Schindeldecker M, Louisa Urbansky L, Berndt K, Sven Gerber T, Lang H, Lotz J, Lackner KJ, Roth W, et al. Comprehensive clinicopathologic study of alpha fetoprotein-expression in a large cohort of patients with hepatocellular carcinoma. *Int J Cancer.* 2022;150(6):1053–1066. doi:10.1002/ijc.33898.
23. Friemel J, Rechsteiner M, Frick L, Böhm F, Struckmann K, Egger M, Moch H, Heikenwalder M, Weber A. Intratumor heterogeneity in hepatocellular carcinoma. *Clin Cancer Res.* 2015;21(8):1951–1961. doi:10.1158/1078-0432.CCR-14-0122.
24. de Sostoa J, Alberto Fajardo C, Moreno R, Ramos MD, Farrera-Sal M, Alemany R. Targeting the tumor stroma with an oncolytic adenovirus secreting a fibroblast activation protein-targeted bispecific T-cell engager. *J ImmunoTher Cancer.* 2019;7(1):19. doi:10.1186/s40425-019-0505-4.
25. Maute RL, Gordon SR, Mayer AT, McCracken MN, Natarajan A, Guo Ring N, Kimura R, Tsai JM, Manglik A, Kruse AC, et al. Engineering high-affinity PD-1 variants for optimized immunotherapy and immuno-PET imaging. *Proc Natl Acad Sci U S A.* 2015;112(47):E6506–14. doi:10.1073/pnas.1519623112.
26. Asunao Numata, Akutsu N, Ishigami K, Koide H, Wagatsuma K, Motoya M, Sasaki S, Nakase H, Numata Y. Synergistic effect of IFN- γ and IL-1 β on PD-L1 expression in hepatocellular carcinoma. *Biochem Biophys Rep.* 2022;30:101270. doi:10.1016/j.bbrep.2022.101270.
27. Okada N, Sugiyama K, Shichi S, Shirai Y, Goto K, Sakane F, Kitamura H, Taketomi A. Combination therapy for hepatocellular carcinoma with diacylglycerol kinase alpha inhibition and anti-programmed cell death-1 ligand blockade. *Cancer Immunol Immunother.* 2022;71(4):889–903. doi:10.1007/s00262-021-03041-z.
28. Peng L, Chen X, Shiyang F, Ren E, Liu C, Liu X, Jiang L, Zeng Y, Wang X, Liu G. Surface engineering of oncolytic adenovirus for a combination of immune checkpoint blockade and virotherapy. *Biomater Sci.* 2021;9(22):7392–7401. doi:10.1039/D1BM00928A.
29. Zhang H, Xie W, Zhang Y, Dong X, Liu C, Jing Y, Zhang S, Wen C, Zheng L, Wang H. Oncolytic adenoviruses synergistically enhance anti-PD-L1 and anti-CTLA-4 immunotherapy by modulating the tumour microenvironment in a 4T1 orthotopic mouse model. *Cancer Gene Ther.* 2022;29(5):456–465. doi:10.1038/s41417-021-00389-3.
30. Hendrickson PG, Olson M, Luetkens T, Weston S, Han T, Atanackovic D, Fine GC. The promise of adoptive cellular immunotherapies in hepatocellular carcinoma. *Oncoimmunology.* 2019;9(1):1673129. doi:10.1080/2162402X.2019.1673129.
31. Guo J, Tang Q. Recent updates on chimeric antigen receptor T cell therapy for hepatocellular carcinoma. *Cancer Gene Ther.* 2021;28(10–11):1075–1087. doi:10.1038/s41417-020-00259-4.
32. Mengling W, Huang Q, Xie Y, Xuyi W, Hongbo M, Zhang Y, Xia Y. Improvement of the anticancer efficacy of PD-1/PD-L1 blockade via combination therapy and PD-L1 regulation. *J Hematol Oncol.* 2022;15(1):24. doi:10.1186/s13045-022-01242-2.
33. Liu L, Chen J, Bae J, Huiyu L, Sun Z, Moore C, Hsu E, Han C, Qiao J, Yang-Xin F. Rejuvenation of tumour-specific T cells through bispecific antibodies targeting PD-L1 on dendritic cells. *Nat Biomed Eng.* 2021;5(11):1261–1273. doi:10.1038/s41551-021-00800-2.
34. Willis Grossman Biegert G, Rosewell Shaw A, Suzuki M. Current development in adenoviral vectors for cancer immunotherapy. *Mol Ther Oncolytics.* 2021;23:571–581. doi:10.1016/j.omto.2021.11.014.